Polymer Chemistry

ROYAL SOCIETY OF CHEMISTRY

PAPER

View Article Online
View Journal | View Issue

Cite this: *Polym. Chem.*, 2022, **13**, 3650

Selective ring-opening polymerization of glycidyl esters: a versatile synthetic platform for glycerol-based (co)polyethers†

Shan Liu,‡[a] Lijun Liu,‡[a] Yubo Zhou,[a] Ye Chen[a] and Junpeng Zhao*[a,b]

Linear polyglycerols are highly valued for their excellent hydrophilicity and biocompatibility as well as their multihydroxy nature. We report here a convenient route for the controlled synthesis of polyglycerols through ring-opening polymerization (ROP) of commercialized glycidyl butyrates (GBs). Starting from enantiopure GBs, well-defined poly(glycidyl ester)s with controlled molar mass and stereoregularity are achieved thanks to the chemoselectivity of the bicomponent metal-free catalyst that prevents both transesterification and epimerization. The pendant butyrate groups are readily cleaved by organobase-catalyzed methanolysis, yielding linear polyglycerols that inherit isotacticity and regioregularity from the parent polymers. Copolymerization of *S*GB and propylene oxide occurs in a random manner resulting in a series of narrowly distributed copolyethers with a precisely regulated number of pendant hydroxyl groups to afford tunable aqueous thermosensitivity. The method is further extended to construct polyglycerol-based amphiphilic and double-hydrophilic copolyethers by block copolymerization of *R*GB with *tert*-butyl glycidyl ether and ethylene oxide, respectively.

Received 28th April 2022,
Accepted 20th May 2022

DOI: 10.1039/d2py00551d

rsc.li/polymers

Introduction

Poly(ethylene oxide) (PEO) is the most widely used synthetic polymer in bio-related technologies in virtue of its excellent hydrophilicity and biocompatibility,[1,2] but is intrinsically limited by the low degree of functionality as it usually bears a maximum of two reactive groups at the chain ends for (bio) conjugation or further derivatization.[3] Linear polyglycerol (PGC, also termed polyglycidol) has also attracted much attention as another epoxide-derived hydrophilic polyether, as well as a multifunctional alternative (with one pendant hydroxymethyl group per repeating unit) to PEO.[4–6] It has been reported that PGC exhibits comparable or even superior water-solubility, biocompatibility,[7,8] fouling-resistant ability, *etc.*,[9–11] as compared with PEO, and is therefore considered an ideal complement or replacement in many PEO-dependent applications.[2] For instance, oligoglycerols and their fatty acid esters are approved by the FDA to be used as food and pharmaceutical additives.[12,13] Moreover, the inherent multiple hydroxyl groups of PGC can be chemically modified to incorporate a rich catalogue of reactive pendant groups such as carboxyl, azide, allyl, thiol, *etc.*, thereby facilitating the application of PGC in biomedical areas such as encapsulation, and storage and transport of biomolecules where two or more functions of the polymer are desired.[4,5,14]

Linear PGC, however, has hardly been involved in industrial manufacturing to date (only diglycerol and triglycerol are commercially available) because the direct synthesis of linear PGC from glycidol through ring-opening polymerization (ROP) is enormously challenging (most probably impossible). The inimer nature of glycidol leads only to branched or hyperbranched polyethers.[7,8] Therefore, it becomes indispensable to use hydroxyl-protected glycidol derivatives as monomers. So far, the successful synthesis of well-defined linear PGC has been accomplished by the ROP of trimethylsilyl glycidyl ether, ethoxyethyl glycidyl ether (EEGE) and other acetal-based glycidyl ethers, *tert*-butyl glycidyl ether (^{t}BGE), allyl glycidyl ether, and isopropylidene glyceryl glycidyl ether followed by acid hydrolysis and/or Pd/C hydrogenation of the protective groups to liberate free pendant hydroxyl groups.[4,5,15–23]

Carboxylic ester is another commonly employed protection for hydroxyl groups which can be facilely and, in most cases, quantitatively formed and cleaved. Typically, the radical polymerization of vinyl acetate (VAc) followed by the alkaline hydrolysis of the pendant ester groups of poly(vinyl acetate) is

[a]*Faculty of Materials Science and Engineering, South China University of Technology, Guangzhou 510640, China. E-mail: msjpzhao@scut.edu.cn*
[b]*Guangdong Provincial Key Laboratory of Luminescence from Molecular Aggregates, South China University of Technology, Guangzhou 510640, China*

†Electronic supplementary information (ESI) available: Experimental details, additional SEC traces, and NMR spectra. See DOI: **https://doi.org/10.1039/d2py00551d**

‡These authors contributed equally to this work.

a long-established and industrialized technique to obtain poly (vinyl alcohol) (PVA), the most commercially important water-soluble plastic for large-scale uses (Scheme 1a).[24] As an oxygenated heterochain analog of PVA, however, linear PGC has not been obtained from ester-protected glycidol derivatives, *i.e.* glycidyl (carboxylic) esters. The main reason lies in that carboxylic esters easily undergo side reactions, typically transesterification, under strongly basic or (Lewis) acidic conditions that are usually used for the ROP of epoxides,[25,26] which would cause impaired pendant groups and disordered polyether structures. The only successful example of synthesizing poly(glycidyl esters) may be the selective ROP of glycidyl methacrylate, affording reactive polyethers with pendant methacrylate groups which provide multiple possibilities for post-polymerization modifications and curing.[27–30] Considering that glycidyl esters, including pure enantiomers, may be readily accessible by *e.g.* esterification of glycidol, epoxidation of allyl esters, or substitution of epichlorohydrin by sodium carboxylate,[31,32] and that some are already commercially available, we are interested to pave a new route to linear PGC by exploring the selective ROP of glycidyl esters (Scheme 1b).

Since the initial attempts using alkylaluminum compounds for monomer-activated ROP of various epoxides by Carlotti and Deffieux,[33–35] two-component Lewis pair initiators/catalysts have thrived in the last few decades. The triethylborane (Et_3B)-organobase system, first reported by Feng *et al.*,[36] has been among the most attractive ones in recent years for the ROP of epoxides and copolymerization of epoxides with non-epoxide monomers (*e.g.* cyclic anhydrides and compounds with cumulated double bonds).[37–55] It is usually considered that Et_3B, a metal-free analog to alkylaluminum, acts as both an epoxide activator and an (oxyanionic) chain-end coordinator to ensure greatly enhanced catalytic efficiency and diminish side reactions associated with high basicity and/or high nucleophilicity. It was found that such a Lewis pair with excess Et_3B allows well-controlled and strictly chemoselective (transesterification-free) ROP of epoxide monomers, including ethylene oxide (EO), propylene oxide (PO), glycidyl ethers, *etc.*, in the presence of small-molecule and/or macromolecular carboxylic esters (as the end groups, main-chain components, or solvents).[56–58] We thus envisaged that such a unique character could be utilized for the chemoselective ROP of glycidyl esters with fully suppressed transesterification on the monomer and the polyether pendant groups, so as to facilitate the precise and versatile synthesis of linear PGC and other glycerol-based (hydroxymethyl-carrying) copolyethers.

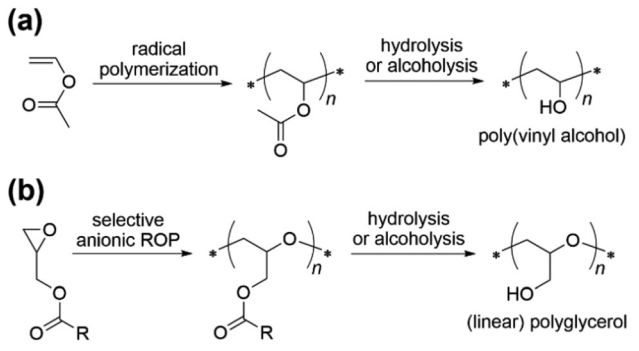

Scheme 1 Comparative illustration of the well-established synthetic route to PVA through the radical polymerization of VAc and the route proposed in this study for linear PGC through the selective anionic ROP of glycidyl carboxylic esters.

Results and discussion

Enantiopure glycidyl butyrates (GBs), including (*R*)-(−)-glycidyl butyrate (*R*GB) and (*S*)-(+)-glycidyl butyrate (*S*GB), can be produced on a large scale by the enzymatic resolution of their racemic mixtures.[31,59,60] Commercially available *R*GB and *S*GB are thus selected as representative glycidyl ester monomers in this study. The combination of a phosphazene base (^{t}BuP$_2$) and excess Et_3B is employed as the bicomponent metal-free catalyst with benzyl alcohol (BA) as the initiator (Scheme 2a and Table 1).[61] The ROP of *R*GB is conducted for the first time at room temperature (RT; 23–25 °C) in bulk with a target degree of polymerization (DP) of 70 and a low catalyst loading ($[RGB]_0/[BA]_0/[^tBuP_2]/[Et_3B]$ = 70/1/0.05/0.15) which was previously shown to lead to efficient and transesterification-free ROP of epoxides in the presence of carboxylic esters.[56–58] However, the ROP proceeds much slower in this case as at least 9 days are needed to reach full monomer conversion as shown by the ^{1}H NMR spectrum of the withdrawn crude products (entry 1 in Table 1, Fig. S1†), which is most probably due to the lower concentration of the epoxy group in bulk caused by the relatively higher molecular weight of GB and/or the higher steric hindrance of the propagating hydroxy species as compared with representative epoxide monomers (*e.g.* EO and PO).[61] One benefit of using this bicomponent catalyst is that the catalytic activity can be finely regulated by varying the ratio and amounts of the Lewis acid and/or base.[57] Indeed, adding more Et_3B to increase the loaded ratio of $[^tBuP_2]/[Et_3B]$ from 1/3 to 1/5 leads to a markedly higher polymerization rate as the monomer is fully consumed in 56 h (entry 2 in Table 1). Full monomer conversions are also achieved in 36 and 72 h when the target DP is varied to 30 and 280, respectively (entries 3 and 4 in Table 1). Note that the overall catalyst loading is quadrupled for the highest DP to ensure an acceptable reaction time.

Size exclusion chromatography (SEC) conducted in tetrahydrofuran (THF) shows unimodal and narrow molar mass distribution ($Đ_M$ < 1.15) for lower target DPs (30 and 70), and a small shoulder towards the high-molar-mass side for the highest DP (280) most probably caused by adventitious water which acts as a difunctional initiator (Fig. 1a). The apparent number-average molar mass ($M_{n,SEC}$) continuously increases with an increase in the target DP, indicating that the molar mass of the ROP product is controlled by the feed ratio of the monomer and the initiator. The deviation of $M_{n,SEC}$ from the theoretical molar mass ($M_{n,th}$) is in part due to the use of polystyrene (PS) standards for calibration. For the largest DP,

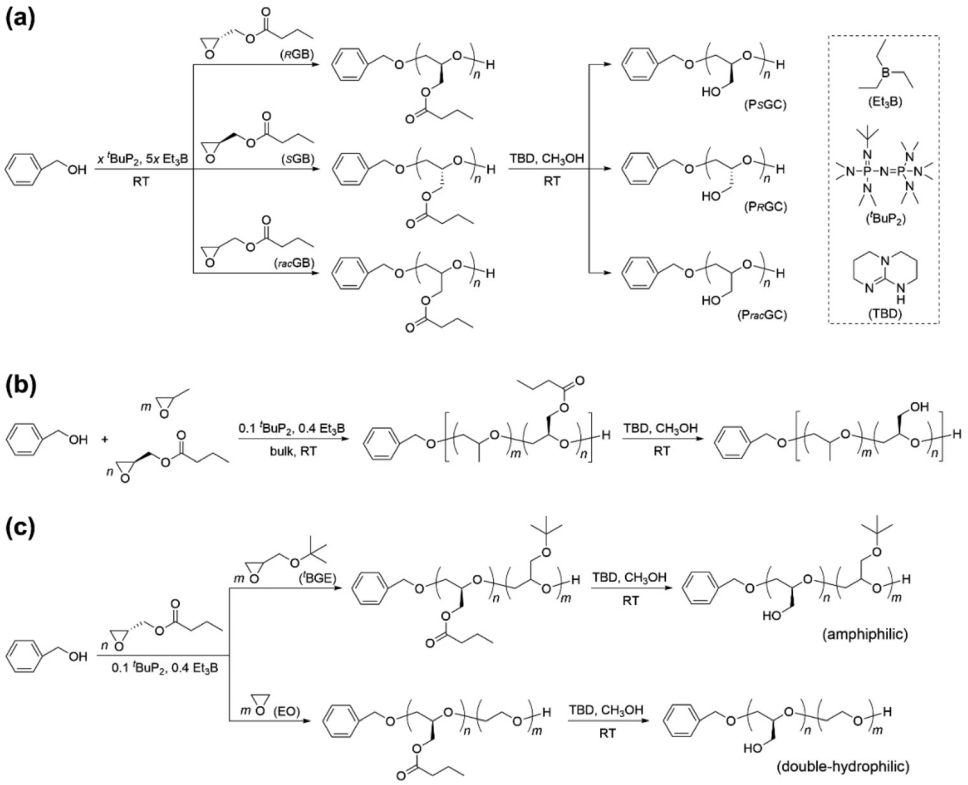

Scheme 2 (a) General scheme for the chemo- and regioselective ROP of GBs catalyzed by ^{t}BuP$_2$-Et$_3$B and initiated by BA followed by methanolysis to obtain (stereoregular) linear PGCs. (b) Synthesis of P(PO-*co*-*R*GC) with tunable aqueous thermosensitivity by the random copolymerization of PO and *S*GB followed by the methanolysis of the pendant butyrate groups. (c) Synthesis of amphiphilic/double-hydrophilic PSGC-*b*-P^{t}BGE/PSGC-*b*-PEO by the block copolymerization of *R*GB and ^{t}BGE/EO *via* sequential monomer addition followed by the methanolysis of the pendant butyrate groups.

Table 1 Reaction conditions and results of the metal-free (co)polymerization of GBs[a]

Entry	Mon.	$[Mon.]_0/[init.]_0/[^tBuP_2]/[Et_3B]$[b]	Time (h)	$M_{n,th}$[c] (kg mol^{-1})	$M_{n,NMR}$[d] (kg mol^{-1})	$M_{n,SEC}$[e] (kg mol^{-1})	$Đ_M$[e]
1	$_R$GB	70/1/0.05/0.15	220	10.2	9.9	6.7	1.15
2	$_R$GB	70/1/0.05/0.25	56	10.2	10.5	6.9	1.12
3	$_R$GB	30/1/0.05/0.25	36	4.4	4.5	3.9	1.09
4	$_R$GB	280/1/0.2/1.0	72	40.5	40.6	15.3	1.13
5	$_S$GB	30/1/0.05/0.25	36	4.4	4.5	4.0	1.08
6	$_S$GB	70/1/0.05/0.25	56	10.2	10.6	7.1	1.15
7	$_S$GB	280/1/0.2/1.0	72	40.5	41.6	19.3	1.09
8[a]	$_R$GB	30/1/0.1/0.5	36	4.5	4.5	4.3	1.09
9[a]	$_R$GB	280/1/0.2/1.0	72	40.5	40.5	37.9	1.06
10	*rac*GB	70/1/0.05/0.25	56	10.2	10.8	7.4	1.16
11[f]	PO + $_S$GB	95/5/1/0.1/0.4	18	6.3	6.4	9.2	1.06
12[f]	PO + $_S$GB	90/10/1/0.1/0.4	18	6.8	6.8	9.7	1.07
13[f]	PO + $_S$GB	80/20/1/0.1/0.4	18	7.6	7.5	9.8	1.06
14[f]	PO + $_S$GB	50/50/1/0.1/0.4	18	10.2	10.8	10.5	1.09
15[g]	$_R$GB + ^{t}BGE	70/70/1/0.1/0.4	48 + 48	19.3	18.9	13.0	1.09
16[g]	$_R$GB + EO	70/120/1/0.1/0.4	48 + 5	15.5	16.1	22.2	1.15

[a] Performed at RT in bulk with BA or BDM (for entries 8 and 9) as the initiator. Monomer conversion reaches 100% in all cases. [b] Molar feed ratio of the monomer, initiator, ^{t}BuP$_2$, and Et$_3$B. [c] Theoretical number-average molar mass calculated from the feed ratio of the monomer and initiator. [d] Calculated from the ^{1}H NMR spectrum of the isolated product. [e] Apparent number-average molar mass and molar mass distribution determined by SEC in THF (35 °C, PS standards). [f] Random copolymerization of PO and *S*GB. [g] Block copolymerization of *R*GB and ^{t}BGE/EO by sequential monomer addition. For entry 16, SEC is performed in DMF (50 °C, PS standards).

the large deviation may also be caused by protic impurities such as glycidol and butyric acid, in addition to water, which add to the total amount of initiators. Similar SEC results are obtained by the ROP of *S*GB performed under the same conditions and using the same target DPs (entries 5–7 in Table 1; Fig. 1b).

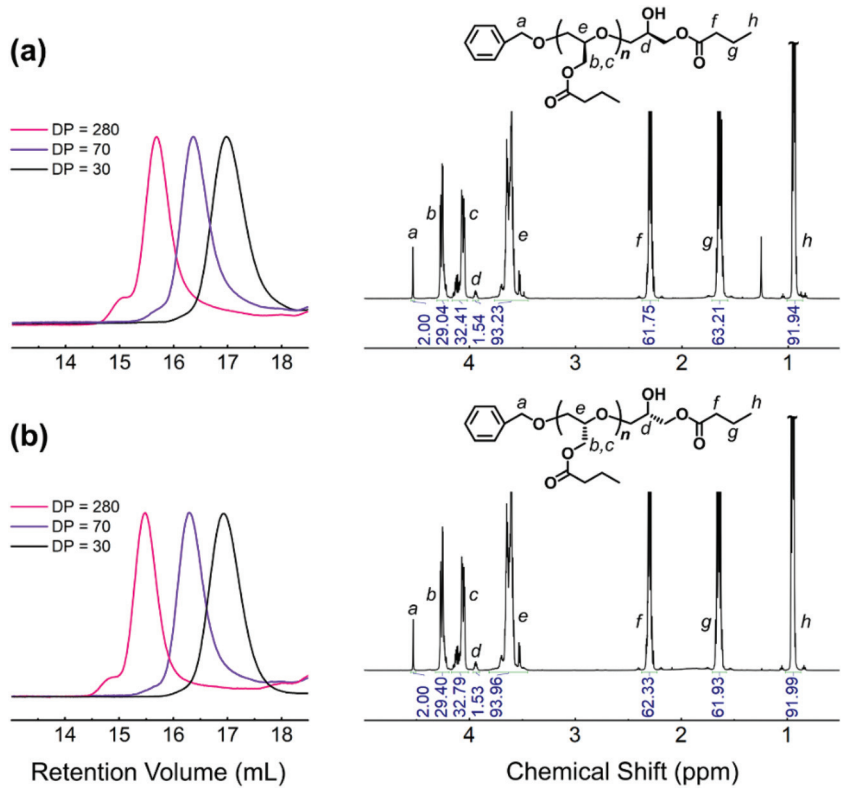

Fig. 1 Left: SEC traces (RI signals, THF, 35 °C) of the crude products of the chemoselective ROP of *R*GB (a) and *S*GB (b) with different target DPs (entries 2–7 in Table 1). Right: ^{1}H NMR spectra (in $CDCl_3$) of the isolated P*R*GB (a) and P*S*GB (b) with a DP of 30.

The well-defined structures of P*R*GB and P*S*GB are identified in ^{1}H NMR and ^{13}C NMR spectra which exhibit all the expected signals of the α-end benzyloxyl (derived from BA), hydroxyl-neighboring methine (at the ω-end), aliphatic ether methylenes and methines (in the polyether backbone), and pendant butyrate groups (Fig. 1 and S2, S3†). The number-average molar mass ($M_{n,NMR}$) calculated by comparison between the signal integrals of PGB main body and α-end methylene conforms well with $M_{n,th}$. The absence of the proton signals of carboxylic esters derived from secondary alcohols, *e.g.* $-CH_2CH(CH_2OCOC_3H_7)OCOC_3H_7$ which would have appeared at *ca.* 5.0 ppm,[25] together with the low $Đ_M$, rules out the possibility of transesterification between the propagating hydroxy chain end and the ester groups on the polymer pendants or the unreacted monomers even with the highest targeted DPs (Fig. S4 and S5†). Therefore, it is confirmed that the controlled and chemoselective ROP of GBs can be achieved with an acid-excess bicomponent metal-free catalyst. It is noted that the number of hydroxyl-neighboring methines at the ω-end is larger than that of BA-derived α-end methylenes according to the integrals of the corresponding proton signals, indicating the existence of impurities acting as extra initiators.

1,4-Benzenedimethanol (BDM) is used as a difunctional initiator for the ROP of *R*GB with a low target DP (entry 8 in Table 1). Controlled molar mass, low $Đ_M$, and high end-group fidelity are achieved as evidenced by SEC and ^{1}H NMR results (Fig. 2a). The matrix assisted laser desorption/ionization time of flight mass spectrometry (MALDI-TOF MS) spectrum of the isolated product depicts a single mass population with a constant interval of 144.2 Da (the molecular weight of *R*GB), further verifying the achievement of the expected BDM-centered α,ω-dihydroxyl P*R*GB structure and that the butyrate groups remain intact during the ROP. In comparison with the SEC profile containing a shoulder peak shown by BA-initiated PGBs with the highest DP, a monomodal and narrow distribution is obtained with BDM as the initiator (entry 9 in Table 1), which is supportive of the presence of a trace amount of water acting as a difunctional initiator in the previous case (Fig. S6†). It needs to be noted that this experiment was done with thoroughly purified *R*GB by prolonged drying several times over CaH_2 and distillation. Therefore, the distinctly increased molar mass of P*R*GB clearly shows that the large deviation between the measured and theoretical molar masses observed above for DP = 280 (entries 4 and 7) is due to the presence of impurities in the monomer acting as extra initiators. The racemic mixture of *R*GB and *S*GB (*rac*GB) is also polymerized with a target DP of 70 which shows a similar reaction time and results in enantiopure monomers (entry 10 in Table 1).

Since there are two Lewis basic sites in one monomer, we are interested to understand the interactions between Et_3B and

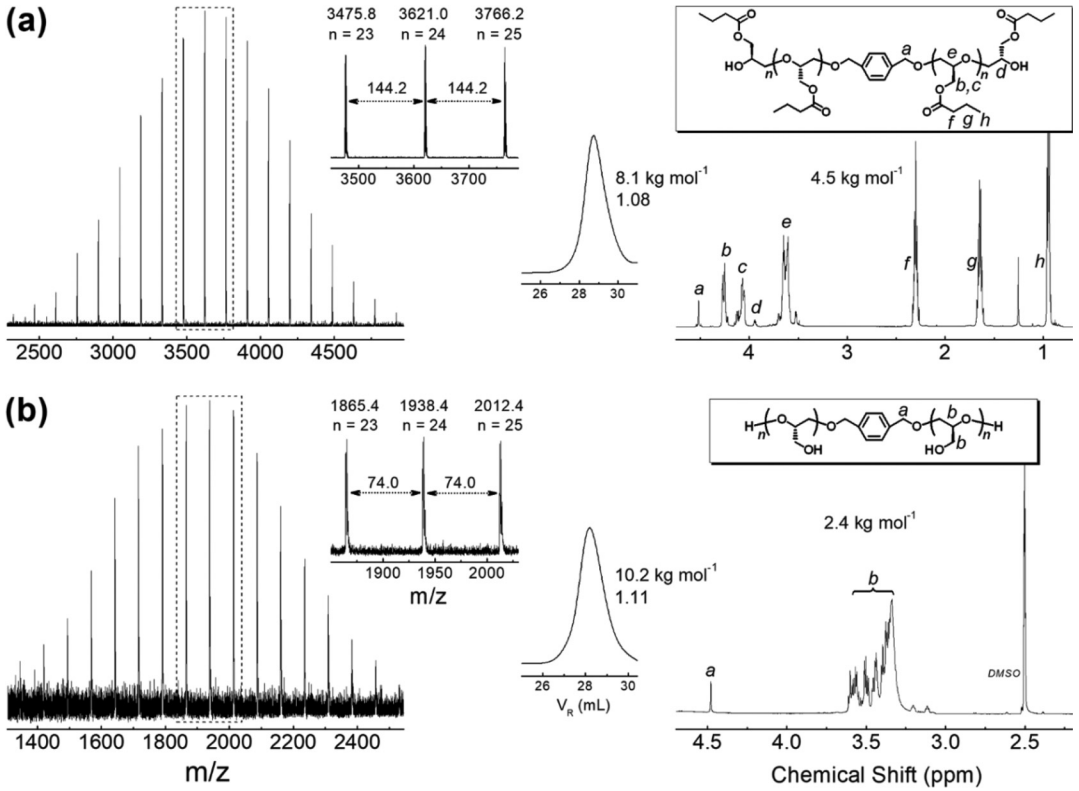

Fig. 2 MALDI-TOF MS spectra (left), SEC traces (middle; RI signals, DMF, 50 °C, PS standards; with $M_{n,SEC}$ and $Đ_M$ noted), and ^{1}H NMR spectra (right; with $M_{n,NMR}$ noted) taken in $CDCl_3$ (upper) or DMSO-d_6 (lower) of (a) BDM-initiated P*R*GB (entry 8 in Table 1; DP = 30) and (b) the P*S*GC obtained after methanolysis. Mass signals in the MALDI-TOF MS spectra correspond to polymers ionized by sodium cations. The calculated masses of (a) [BDM-*R*GB$_{24}$]Na$^+$ and (b) [BDM-*S*GC$_{24}$]Na$^+$ are 3621.2 and 1939.1 Da, respectively.

the oxygen atoms in the epoxy ring and the pendant ester group by conducting DFT calculations (Fig. S7†). A minimum value is observed in a potential energy surface for the interaction between Et_3B and the epoxy group, while the interaction energy of Et_3B and the ester carbonyl group decreases monotonically as the atom distance increases. It is thus suggested that Et_3B preferentially interacts with epoxides and the plausible conjugation between Et_3B and carbonyl is unfavorable, probably due to the steric effect. Such results are consistent with our earlier assumption that the relatively slow polymerization rate with a low amount of Et_3B is likely ascribed to the bulkiness and low bulk concentration of GBs, rather than a competitive interaction of Et_3B by pendant ester groups.

Next, organobase-catalyzed methanolysis of PGBs is performed to liberate the pendant hydroxyl groups and afford linear PGCs (Scheme 2a). ^{1}H NMR analysis shows that methanolysis is completed in 12 h at RT by the addition of an organobase, (1,5,7-triazabicyclo[4.4.0]dec-5-ene (TBD), used in a small amount (5% of the ester groups). The SEC peak obtained in *N*,*N*-dimethylformamide (DMF), however, reveals a distinct shift to the low-elution-volume (high-molar-mass) side after methanolysis, which is probably because PGCs are more solvophilic than the parent PGBs in DMF. Narrow and unimodal distributions for all PGC samples are maintained (Fig. 2b and S8†), indicating the chemical inertness of the polyether backbone under the methanolysis conditions. Note that using DMF as the mobile phase and PS samples as the standards for PGB and PGC may have caused a considerable overestimation of their molar masses. However, DMF is the only one among commonly used SEC eluents that can well-dissolve both PGB and PGC for making comparisons before and after methanolysis. The disappearance of the signals of carbonyl-neighboring *n*-propyl and pendant methylene groups (–CH_2OCOC$_3H_7$), the appearance of hydroxymethyl signals (–CH_2OH, 3.2–3.5 ppm) generated in the ^{1}H NMR spectrum of the isolated product, and the fitting measured molar masses (*e.g.*, $M_{n,NMR}$ = 2.4 kg mol^{-1}, $M_{n,th}$ = 2.4 kg mol^{-1} in Fig. 2b) further indicate the complete removal of the butyryl groups and the successful transformation of PGBs into PGCs with the same DP. The expected linear PGC structure is also confirmed by the MALDI-TOF MS spectrum which is the absence of the products caused by incomplete methanolysis or by other side reactions. Owing to the poor solubility of PGC in common organic solvents such as THF, 2-methyl THF, acetone, ethyl acetate, dichloromethane, and chloroform, the generated PGC is easily isolated by precipitation with the catalyst residuals and small-molecule byproducts (*i.e.* methyl butyrate), which are comple-

tely removed. Also note that similar results are obtained when 1,8-diazabicyclo[5.4.0]undec-7-ene (DBU) instead of TBD is used as the methanolysis catalyst with the same loaded amount and reaction time (Fig. S9†).

The microstructures of PGBs and the corresponding PGCs with a DP of 70 derived from *R*GB, *S*GB, and *rac*GB (products in entries 2, 6, and 10 in Table 1) are analyzed by the use of their ^{13}C NMR spectra. P*R*GB and P*S*GB present singlet signals for the backbone methylene and methine carbons and the pendant methylene carbon adjacent to the backbone, indicating that the epimerization of the enantiopure GBs is absent during the ROP so that highly isotactic structures are achieved. Also, such a result strongly suggests that the opening of the epoxy ring occurs selectively through sterically favored β-scission so that chiral configuration inversion is minimal.[62] In this way, isotactic PGBs with stringent head-to-tail regioregularity are obtained. On the other hand, P*rac*GB shows distinctly broader and multiple peaks for the same carbons (Fig. 3a), indicating that *R*GB and *S*GB copolymerize in a random manner leading to an atactic structure. The stereoregularity difference between P*R*GB/P*S*GB and P*rac*GB is also implied by the forms of the isolated polymer samples. While P*rac*GB remains as a viscous liquid under all storage conditions, P*R*GB and P*S*GB turn into white solids when stored in a fridge at 4 °C or −20 °C or even at RT with an adequate time. The (semi)crystalline feature of the isotactic PGBs is also revealed by the wide-angle X-ray diffraction profiles of the solidified samples which exhibit five strong diffraction peaks (Fig. S10†). Differential scanning calorimetry (DSC) shows glass transition temperatures (T_gs) of −57.3 °C, −55.7 °C and −63.9 °C for P*R*GB, P*S*GB and P*rac*GB, and melting points (T_ms) of 38.7 °C and 40.4 °C for P*R*GB and P*S*GB, respectively (Fig. S10†). Note that T_m is taken from the first heating run owing to the slow recrystallization of the melted PGBs. However, a stereocomplex may not be formed when P*R*GB and P*S*GB are mixed in a 1 : 1 mass ratio as suggested by DSC results. This is understood as a result of the bulky pendant butyrate group which hinders the ordered co-crystallization of P*R*GB and P*S*GB segments. Much effort is being made to better reveal and understand the crystallinity of stereoregular PGBs and other poly(glycidyl esters).

The stereoregularity of the parent PGBs is fully inherited by the PGCs obtained after methanolysis, as revealed by the singlet signals of P*S*GC/P*R*GC and the split signals of P*rac*GC in their ^{13}C NMR spectra, especially for the main-chain methine carbons (Fig. 3b). The obtained linear P*S*GC and P*R*GC, though highly stereo- and regio-regular, appear to be amorphous under all storage conditions (also indicated by DSC measurements, Fig. S11†), which is in accordance with previous reports.[4,63,64] No stereocomplexation is suggested for the P*R*GC and P*S*GC blend either. In fact, the properties of stereoregular PGCs are highly under-investigated in the literature.[63,64] Therefore, our method provides a useful tool to exploit this specific area, given that there are well-established synthetic routes to enantiopure GBs.[31,59,60]

The statistical copolymerization of PO and *S*GB is carried out aiming at P(PO-*co*-*S*GC)s with an adjustable number of pendant hydroxyl groups and properties. The molar feed ratio of the monomers (in total), BA, and the catalytic components ($[M]_0/[BA]_0/[^tBuP_2]/[Et_3B]$) is fixed at 100/1/0.1/0.4 to target a constant DP of 100, while the fraction of *S*GB in the mixed monomer is varied to be 5%, 10%, 20%, and 50% (Scheme 2b, entries 11–14 in Table 1). Both monomers are fully consumed within 18 h in all cases. SEC presents narrow and unimodal molar mass distributions, indicating that the copolymerization is well-controlled. The expected P(PO-*co*-*S*GB) structures with molar masses and comonomer compositions agreeing well with the theoretical values are confirmed by ^{1}H NMR data (Fig. 4 and S12–S14†). Plots of monomer conversion versus reaction time obtained from the experiment with equally loaded molar amounts of PO and *S*GB (entry 14 in Table 1) show that the two monomers react at comparable rates (with PO incorporated in the copolymer slightly faster) and that the molar mass of the copolyether increases steadily with a low $Đ_M$ maintained throughout the copolymerization (Fig. S15†). In contrast to PPO and P*S*GB homopolymers, the ^{13}C NMR spec-

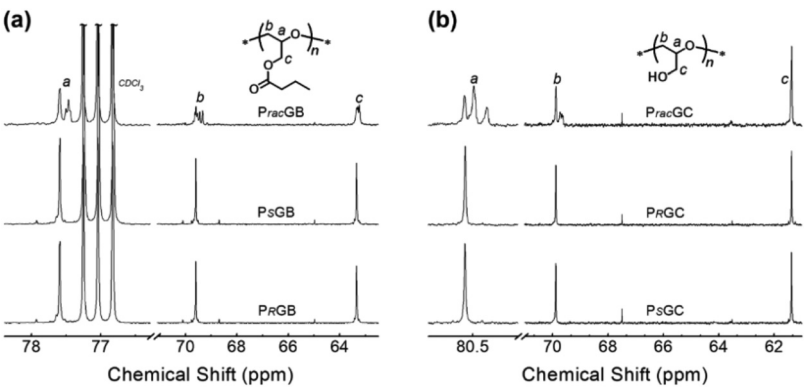

Fig. 3 (a) ^{13}C NMR spectra (in $CDCl_3$) of P*R*GB, P*S*GB, and P*rac*GB with a DP of 70 (the isolated products in entries 2, 6, and 10 in Table 1, respectively). (b) ^{13}C NMR spectra (in DMSO-d_6) of the corresponding P*S*GC, P*R*GC, and P*rac*GC obtained by TBD-catalyzed methanolysis and precipitation in THF.

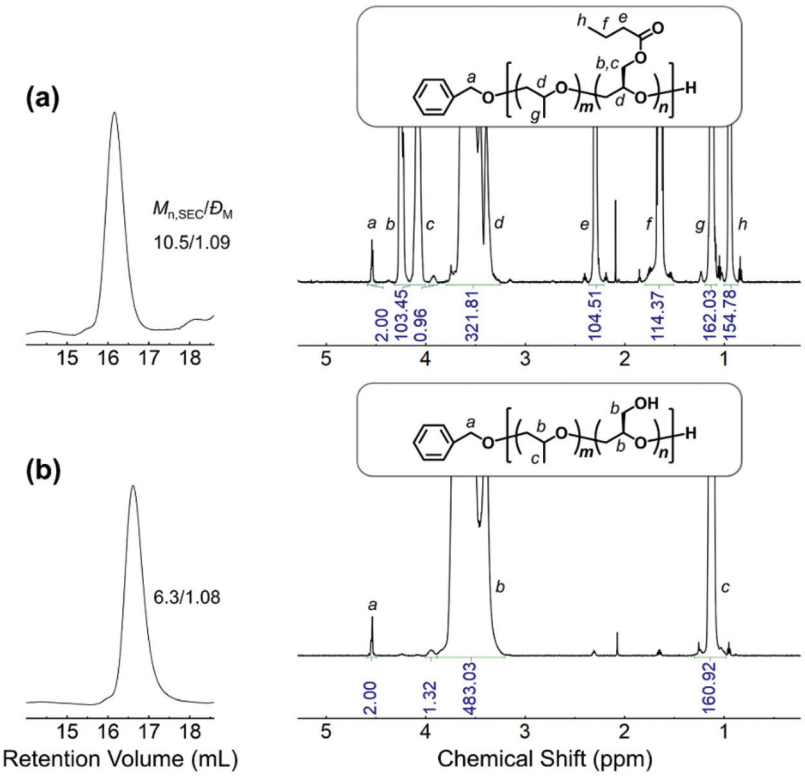

Fig. 4 SEC traces (RI signals, THF, 35 °C, PS standards) and ^{1}H NMR spectra (in $CDCl_3$) of (a) P(PO_{50}-*co*-*S*GB_{50}), corresponding to entry 14 in Table 1, and (b) P(PO_{50}-*co*-*R*GC_{50}) obtained after methanolysis treatment.

trum of P(PO_{50}-*co*-*S*GB_{50}) displays evidently broadened and split signals especially for the backbone methine and methylene carbons of the *S*GB units, indicating the altered chemical environment of these carbon atoms (Fig. S16†). An integral ratio of 0.26 is obtained for the *S*GB*S*GB*S*GB linkage, which is very close to that calculated for a perfect statistical binary copolymerization reaction ([*S*GB*S*GB*S*GB] = 0.25). These results support the achievement of well-defined P(PO-*co*-*S*GB) with a highly random sequence distribution of the two monomeric units.

Methanolysis of the copolyethers is conducted in the same manner as described above for PGBs, with 5 mol% of TBD, relative to the ester groups, as the transesterification catalyst. A complete transformation of the pendant butyrates into hydroxymethyl groups and achievement of well-defined P(PO-*co*-*R*GC)s with total DPs and low $Đ_M$s, and compositions of the two monomeric units inherited from the parent P(PO-*co*-*S*GB)s are confirmed by SEC and ^{1}H NMR data (Fig. 4 and S12–S14†). While the P(PO-*co*-*S*GB) precursors do not dissolve in water regardless of temperature and *S*GB contents, the hydroxyl-liberated P(PO-*co*-*R*GC)s are all able to form homogeneous and transparent water solutions after being kept in a fridge (4 °C) for 2 h at a concentration of 1.0 mg mL^{-1}. The aqueous thermosensitivity of the copolyethers is investigated by temperature-dependent light transmittance (turbidity) experiments. P(PO-*co*-*R*GC)s with the molar fractions of *R*GC units being 5%, 10%, and 20%, respectively, exhibit lower critical solution temperatures (LCSTs) of 15 °C, 21 °C, and 33 °C at 50% transmittance during the heating process (Fig. 5). Clearly, the hydrophilicity of the copolyether enhances as more *R*GC units are incorporated. The solution of P(PO-*co*-*R*GC) with 50 mol% of *R*GC units shows a transparent solution in the whole range of temperatures investigated with no LCST being observed.

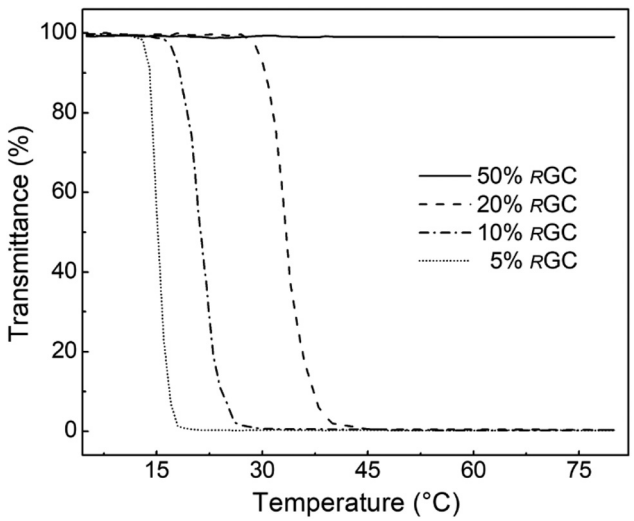

Fig. 5 Temperature dependence of light (λ = 600 nm) transmittance given by the 1.0 mg mL^{-1} aqueous solutions of P(PO-*co*-*R*GC)s with varying molar fractions of *R*GC units (total DP = 100).

Therefore, our method fulfils the controlled synthesis of multifunctional copolyethers with randomly distributed pendant hydroxyl groups and readily tunable aqueous thermosensitivity, similar to the previously reported (cesium hydroxide)-catalyzed copolymerization of PO and EEGE followed by acid hydrolysis.[65]

The utility of glycidol esters for the construction of glycerol-based polyether structures is further addressed by the block copolymerization of *R*GB with ^{t}BGE or EO *via* sequential monomer addition, followed by methanolysis treatment of the P*R*GB block (Scheme 2c; entries 15 and 16 in Table 1). The target DP for P*R*GB is 70 in both cases and 70/120 for P^{t}BGE/PEO. The livingness of the BA-initiated ROP of the epoxides, catalyzed by the acid-excess metal-free Lewis pair ($[BA]_0/[^tBuP_2]/[Et_3B]$ = 1/0.1/0.4), and the formation of P*R*GB-*b*-P^{t}BGE and P*R*GB-*b*-PEO diblock copolymers are demonstrated by the full conversion of the monomers and the increase of molar mass after the addition of the second monomer (Fig. 6). A protrusion to the low-molar-mass side is observed in the SEC peak of P*R*GB-*b*-PEO, which may indicate that the initiation of the ROP of EO by the secondary hydroxyl group at the P*R*GB end is slower than the propagation of the PEO chain with a primary hydroxy active species. This issue would be circumvented if the order of monomer addition was reversed as we observed previously in the block copolymerization of EO and PO.[61] The methanolysis occurs selectively and completely on the P*R*GB blocks for both P*R*GB-*b*-P^{t}BGE and P*R*GB-*b*-PEO as evidenced by SEC and ^{1}H NMR results (Fig. S17 and S18†), leading to the expected P*S*GC-*b*-P^{t}BGE and P*S*GC-*b*-PEO diblock copolymers with fully inherited block lengths of their precursors. The amphiphilic and double-hydrophilic natures of these PGC-based block copolymers, together with the multifunctional and biocompatible features of the PGC blocks, may forge them into useful building materials for *e.g.* nanosized carriers and controlled release systems.

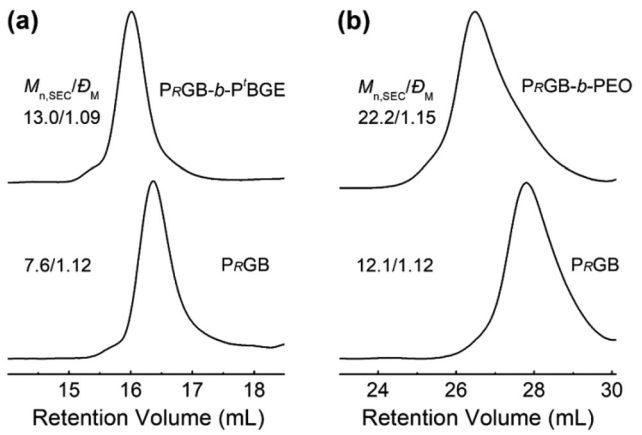

Fig. 6 (a) SEC traces (THF, 35 °C, RI signals, PS standards) of the P*R*GB precursor and the P*R*GB-*b*-P^{t}BGE diblock copolymer (crude products, entry 15 in Table 1). (b) SEC traces (DMF, 50 °C, RI signals, PS standards) of the P*R*GB precursor and P*R*GB-*b*-PEO diblock copolymer (crude products, entry 16 in Table 1).

Conclusions

In summary, we have shown that commercially available and enantiopure glycidol carboxylic esters, *i.e. R*GB and *S*GB, and their racemic mixture (*rac*GB), can undergo chemoselective ROP using an alcoholic initiator and a bicomponent Lewis pair type metal-free catalyst comprising a strong phosphazene base ($^tBuP_2$) and excess Et_3B. Potential side reactions including transesterification and epimerization are fully suppressed so that well-defined and tacticity-controlled polyethers bearing one carboxylic ester pendant group per repeating unit are readily achieved. The pendant butyrate groups can be completely and selectively cleaved by methanolysis catalyzed by an organobase (TBD) to afford linear PGCs with a controlled molar mass, a low molar mass distribution, and high regio- and stereoregularity. GBs can also copolymerize with PO in a highly random manner and with ^{t}BGE/EO in a one-pot sequential manner to afford, respectively, random and block copolymers with controlled compositions. TBD-catalyzed methanolysis also occurs selectively on pendant butyrate groups for these copolymers, resulting in glycerol-based random copolyethers with tunable aqueous thermosensitivity and block copolyethers with amphiphilic and double-hydrophilic nature. Therefore, our study shows that metal-free selective ROP of GB followed by organobase-catalyzed alcoholysis can serve as a useful alternative to the previously established methods based on *e.g.* alkali alcoholate or (onium alkoxide)-aluminum catalyzed ROP of EEGE (an acetal-protected glycidol monomer) and acid hydrolysis of PEEGE for the synthesis of well-defined linear PGC. The commercial availability and well-established synthetic routes for GBs, especially the enantiopure ones, may facilitate the large-scale production of (stereoregular) linear PGCs. Also, the controlled and chemoselective synthesis of GB-based (co)polyethers may be extended to other glycidol esters to create a new subcatalog of aliphatic polyethers with multiple functionalities and new properties.

Author contributions

S. L. and L. L. contributed equally to this work.

Conflicts of interest

There are no conflicts to declare.

Acknowledgements

The financial support from the National Natural Science Foundation of China (52022031, 21734004, 21971075) and the Fund of Guangdong Provincial Key Laboratory of Luminescence from Molecular Aggregates (2019B030301003) is acknowledged.

References

1 J. Herzberger, K. Niederer, H. Pohlit, J. Seiwert, M. Worm, F. R. Wurm and H. Frey, *Chem. Rev.*, 2016, **116**, 2170–2243.
2 K. Knop, R. Hoogenboom, D. Fischer and U. S. Schubert, *Angew. Chem., Int. Ed.*, 2010, **49**, 6288–6308.
3 B. Obermeier, F. Wurm, C. Mangold and H. Frey, *Angew. Chem., Int. Ed.*, 2011, **50**, 7988–7997.
4 A. Thomas, S. S. Müller and H. Frey, *Biomacromolecules*, 2014, **15**, 1935–1954.
5 H. Keul and M. Möller, *J. Polym. Sci., Part A: Polym. Chem.*, 2009, **47**, 3209–3231.
6 H. Zhang and M. W. Grinstaff, *Macromol. Rapid Commun.*, 2014, **35**, 1906–1924.
7 R. K. Kainthan, J. Janzen, E. Levin, D. V. Devine and D. E. Brooks, *Biomacromolecules*, 2006, **7**, 703–709.
8 M. Imran ul-haq, B. F. Lai, R. Chapanian and J. N. Kizhakkedathu, *Biomaterials*, 2012, **33**, 9135–9147.
9 M. Wyszogrodzka and R. Haag, *Langmuir*, 2009, **25**, 5703–5712.
10 M. Weinhart, I. Grunwald, M. Wyszogrodzka, L. Gaetjen, A. Hartwig and R. Haag, *Chem. – Asian J.*, 2010, **5**, 1992–2000.
11 M. Weinhart, T. Becherer, N. Schnurbusch, K. Schwibbert, H. J. Kunte and R. Haag, *Adv. Eng. Mater.*, 2011, **13**, B501–B510.
12 H. Frey and R. Haag, *Rev. Mol. Biotechnol.*, 2002, **90**, 257–267.
13 M. Calderon, M. A. Quadir, S. K. Sharma and R. Haag, *Adv. Mater.*, 2010, **22**, 190–218.
14 Z. Li and Y. Chau, *Bioconjugate Chem.*, 2009, **20**, 780–789.
15 M. Erberich, H. Keul and M. Möller, *Macromolecules*, 2007, **40**, 3070–3079.
16 D. Taton, A. Le Borgne, M. Sepulchre and N. Spassky, *Macromol. Chem. Phys.*, 1994, **195**, 139–148.
17 J. Song, L. Palanikumar, Y. Choi, I. Kim, T.-Y. Heo, E. Ahn, S.-H. Choi, E. Lee, Y. Shibasaki, J.-H. Ryu and B.-S. Kim, *Polym. Chem.*, 2017, **8**, 7119–7132.
18 E. Hwang, K. Kim, C. G. Lee, T.-H. Kwon, S.-H. Lee, S. K. Min and B.-S. Kim, *Macromolecules*, 2019, **52**, 5884–5893.
19 J. Baek, M. Kim, Y. Park and B.-S. Kim, *Macromol. Biosci.*, 2021, **21**, 2100251.
20 A. Dworak, I. Panchev, B. Trzebicka and W. Walach, *Macromol. Symp.*, 2000, **153**, 233–242.
21 M. Gervais, A.-L. Brocas, G. Cendejas, A. Deffieux and S. Carlotti, *Macromolecules*, 2010, **43**, 1778–1784.
22 M. Gervais, A.-L. Brocas, G. Cendejas, A. Deffieux and S. Carlotti, *Macromol. Symp.*, 2011, **308**, 101–111.
23 F. Wurm, J. Nieberle and H. Frey, *Macromolecules*, 2008, **41**, 1909–1911.
24 V. Goodship and D. Jacobs, *Polyvinyl alcohol: materials, processing and applications*, Smithers rapra technology, 2009.
25 S. Hu, J. Zhao and G. Zhang, *ACS Macro Lett.*, 2015, **5**, 40–44.
26 J. P. Zhao, D. Pahovnik, Y. Gnanou and N. Hadjichristidis, *Macromolecules*, 2014, **47**, 1693–1698.
27 A. L. Labbé, A.-L. Brocas, E. Ibarboure, T. Ishizone, A. Hirao, A. Deffieux and S. P. Carlotti, *Macromolecules*, 2011, **44**, 6356–6364.
28 M. T. Muñoz, M. Palenzuela, T. Cuenca and M. E. Mosquera, *ChemCatChem*, 2018, **10**, 936–939.
29 N. Bicak and B. Karagoz, *Polym. Bull.*, 2006, **56**, 87–93.
30 B. Karagoz and N. Bicak, *Eur. Polym. J.*, 2008, **44**, 106–112.
31 Y. J. K. Araujo, N. P. Avvari, D. R. Paiva, D. P. D. Lima and A. Beatriz, *Tetrahedron Lett.*, 2015, **56**, 1696–1698.
32 P. Muppa, R. Postma, C. Schoolderman, S. Rens and K. Stoitsas, *U.S. Patent No* 9174955, 2015.
33 A.-L. Brocas, C. Mantzaridis, D. Tunc and S. Carlotti, *Prog. Polym. Sci.*, 2013, **38**, 845–873.
34 S. P. Carlotti, A. L. Labbé, V. Rejsek, S. P. Doutaz, M. Gervais and A. Deffieux, *Macromolecules*, 2008, **41**, 7058–7062.
35 A. Labbé, S. Carlotti, C. Billouard, P. Desbois and A. Deffieux, *Macromolecules*, 2007, **40**, 7842–7847.
36 D. Zhang, S. K. Boopathi, N. Hadjichristidis, Y. Gnanou and X. Feng, *J. Am. Chem. Soc.*, 2016, **138**, 11117–11120.
37 C.-J. Zhang, H.-Y. Duan, L.-F. Hu, C.-H. Zhang and X.-H. Zhang, *ChemSusChem*, 2018, **11**, 4209–4213.
38 S. K. Boopathi, N. Hadjichristidis, Y. Gnanou and X. Feng, *Nat. Commun.*, 2019, **10**, 293–301.
39 J.-L. Yang, H.-L. Wu, Y. Li, X.-H. Zhang and D. J. Darensbourg, *Angew. Chem., Int. Ed.*, 2017, **56**, 5774–5779.
40 L.-F. Hu, C.-J. Zhang, H.-L. Wu, J.-L. Yang, B. Liu, H.-Y. Duan and X.-H. Zhang, *Macromolecules*, 2018, **51**, 3126–3134.
41 N. G. Patil, S. K. Boopathi, P. Alagi, N. Hadjichristidis, Y. Gnanou and X. Feng, *Macromolecules*, 2019, **52**, 2431–2438.
42 M. Jia, N. Hadjichristidis, Y. Gnanou and X. Feng, *Angew. Chem., Int. Ed.*, 2021, **60**, 1593–1598.
43 M. Jia, N. Hadjichristidis, Y. Gnanou and X. Feng, *ACS Macro Lett.*, 2019, **8**, 1594–1598.
44 Z. Chen, J.-L. Yang, X.-Y. Lu, L.-F. Hu, X.-H. Cao, G.-P. Wu and X.-H. Zhang, *Polym. Chem.*, 2019, **10**, 3621–3628.
45 M. Jia, D. Zhang, G. W. de Kort, C. H. R. M. Wilsens, S. Rastogi, N. Hadjichristidis, Y. Gnanou and X. Feng, *Macromolecules*, 2020, **53**, 5297–5307.
46 V. K. Chidara, S. K. Boopathi, N. Hadjichristidis, Y. Gnanou and X. Feng, *Macromolecules*, 2021, **54**, 2711–2719.
47 C.-J. Zhang, S.-Q. Wu, S. Boopathi, X.-H. Zhang, X. Hong, Y. Gnanou and X.-S. Feng, *ACS Sustainable Chem. Eng.*, 2020, **8**, 13056–13063.
48 L.-F. Hu, D.-J. Chen, J.-L. Yang and X.-H. Zhang, *Molecules*, 2020, **25**, 253–263.
49 B. Zhang, H. Li, H. Luo and J. Zhao, *Eur. Polym. J.*, 2020, **134**, 109820.
50 H. Li, G. He, Y. Chen, J. Zhao and G. Zhang, *ACS Macro Lett.*, 2019, **8**, 973–978.
51 H.-Y. Ji, D.-P. Song, B. Wang, L. Pan and Y.-S. Li, *Green Chem.*, 2019, **21**, 6123–6132.
52 N. Patil, S. Bhoopathi, V. Chidara, N. Hadjichristidis, Y. Gnanou and X. Feng, *ChemSusChem*, 2020, **13**, 5080–5087.

53 J. K. Varghese, N. Hadjichristidis, Y. Gnanou and X. Feng, *Polym. Chem.*, 2019, **10**, 3764–3771.
54 G. W. Yang, Y. Y. Zhang, R. Xie and G. P. Wu, *Angew. Chem., Int. Ed.*, 2020, **59**, 16910–16917.
55 Y.-Y. Zhang, G.-W. Yang and G.-P. Wu, *Synlett*, 2022, **33**, 8–15.
56 Y. Chen, S. Liu, J. Zhao, D. Pahovnik, E. Žagar and G. Zhang, *ACS Macro Lett.*, 2019, **8**, 1582–1587.
57 S. Liu, T. Bai, K. Ni, Y. Chen, J. Zhao, J. Ling, X. Ye and G. Zhang, *Angew. Chem., Int. Ed.*, 2019, **58**, 15478–15487.
58 S. Liu, L. Liu, Y. Chen and J. Zhao, *Chem. Commun.*, 2020, **56**, 12186–12189.
59 W. E. Ladner and G. M. Whitesides, *J. Am. Chem. Soc.*, 1984, **106**, 7250–7251.
60 A. L. Margolin, *Enzyme Microb. Technol.*, 1993, **15**, 266–280.
61 Y. Chen, J. Shen, S. Liu, J. Zhao, Y. Wang and G. Zhang, *Macromolecules*, 2018, **51**, 8286–8297.
62 W.-M. Ren, T.-J. Yue, X. Zhang, G.-G. Gu, Y. Liu and X.-B. Lu, *Macromolecules*, 2017, **50**, 7062–7069.
63 A. Haouet, M. Sepulchre and N. Spassky, *Eur. Polym. J.*, 1983, **19**, 1089–1098.
64 C. C. Price and E. J. Vandenberg, *Coordination polymerization*, Plenum Press, New York, 1983.
65 M. Schömer and H. Frey, *Macromolecules*, 2012, **45**, 3039–3046.